Central European Journal of Energetic Materials
ISSN 1733-7178; e-ISSN 2353-1843

Cent. Eur. J. Energ. Mater. 2026, *23*(1): 19-43; DOI 10.22211/cejem/219995
Article is available in PDF-format, in colour, at:
https://ipo.lukasiewicz.gov.pl/wydawnictwa/cejem-woluminy/vol-23-nr-1/

Research paper

Study on Optimum Composition and Characteristics of Pour-Casting Red Phosphorus Smoke Agents with Different Oxidizers

Jin-Shuh Li[1,*)], **Cheng-Hsiung Peng**[2)], **Kai-Tai Lu**[1)], **Po-Han Chen**[3)]

[1)] *Department of Chemical and Materials Engineering, Chung Cheng Institute of Technology, National Defense University, Taoyuan, 33551, Taiwan, Republic of China*

[2)] *Department of Applied Materials Science and Technology, Minghsin University of Science and Technology, Hsinchu, 30401, Taiwan, Republic of China*

[3)] *Master Program of Chemical Engineering, Chung Cheng Institute of Technology, National Defense University, Taoyuan, 33551, Taiwan, Republic of China*

* *E-mail:* lijinshuh@gmail.com

Abstract: This study used experimental methods to explore the optimum composition and characteristics of pour-casting red phosphorus (RP) smoke agents with KNO_3, MnO_2 or SiO_2 as the oxidizer. Taguchi experimental design method was adopted to design the experimental conditions, and three series of scaled-down test samples were prepared by vacuum pour-casting method in order to analyze the optimum parameter combinations for the minimum average burning rate. The combustion phenomena of these scaled-down test samples were recorded by the visual-image capture system, and the ignition and combustion temperatures were measured by the temperature measurement system. Subsequently, the uniformity of composition distribution, hardness and mechanical strength of three scaled-down test samples prepared with the optimum parameter combination were observed and measured by scanning electron microscopy coupled with energy

dispersive spectroscopy, hardness tester and tensile testing machine. In addition, the vacuum stability tester was used to determine the stability, and the smoke density test chamber was employed to measure the specific optical density of smoke generated by test samples. Finally, the combustion performance of three full-size smoke candles prepared with the optimum parameter combination was measured and compared with that of the smoke candle in the MK 58 smoke marker. The experimental results indicated that three scaled-down test samples prepared with the optimum parameter combination had uniform composition distribution, proper hardness, sufficient strength and ductility to avoid structural damage, and good stability. In addition, the smoke densities generated by the test samples with KNO_3 or MnO_2 as the oxidizer are similar, but they were higher than the smoke density generated by test samples with SiO_2 as the oxidizer. The combustion performance of the full-size RP smoke candles with KNO_3 or MnO_2 as the oxidizer was close to that of the smoke candle in the MK 58 smoke marker. However, the full-size RP smoke candle with SiO_2 as the oxidizer had a longer smoke-generating time but a lower smoke density than the smoke candle in the MK 58 smoke marker.

Keywords: smoke marker, pour-casting, red phosporous, oxidizer, optimum composition, combustion performance

1 Introduction

Smoke markers, also known as marine location markers (MLMs), are used in both military and commercial applications. In military applications, they can be launched by day or night from high-speed aircraft, helicopters or surface ships to provide a visual marker on the sea surface for a range of operations. In commercial applications, they can be used to mark locations on the sea surface for search and rescue operations as well as for training of crew on board [1-4]. The smoke-producing composition used in the smoke marker is designed to generate smoke, and its components mainly include fuel, oxidizer, flame retardant, dye (especially for colored smoke), coolant and binder [5, 6]. The smoke-producing composition is usually placed in a closed can or container. Therefore, it must be easy to generate smoke in the absence of oxygen or air. In other words, the primary pyrotechnic reaction should be self-sustaining [2]. Furthermore, the smoke-producing composition should preferably be able to disperse the smoke slowly over a given period of time to allow identification of the area where the smoke originated.

Phosphorus smokes produced by red phosphorus (RP) and white phosphorus (WP) are often used by the military to protect friendly forces, support deception operations, identify enemy targets and tactical locations, and cover certain

reconnaissance activities, surveillances, and targets from enemy forces. However, WP is highly toxic to the human body, while RP is insoluble in water and is not absorbed by the human body when ingested. In addition, RP is not nearly as reactive as WP, burning particles of WP dispersed by bursting smoke devices, can cause thermal burns. In contrast, the combustion of RP-based compositions in a canister or container is less hazardous to bystanders [7]. Therefore, RP is used in most smoke markers as the main component of the smoke-producing composition. MK 58 smoke marker is a commonly used marine location marker that is 21.5 inches (54.6 cm) long, 5.0 inches (12.7 cm) in diameter and weighs about 12.75 pounds (5.8 kg), and can provide a long-burning, smoke and flame reference-point on the sea surface for 40 to 60 min [8, 9]. The pyrotechnic formulation used for MK 58 smoke marker originally consists of 53% RP, 34% MnO_2, 7% Mg, 3% ZnO and 3% linseed oil (LO) [10, 11]. Regarding the smoke-producing mechanism of MK 58 smoke marker, the first is the reaction between MnO_2 and Mg, which can generate enough heat to sublimate RP, and then the sublimated RP comes into contact with the atmosphere and undergoes a combustion reaction to produce phosphorus smoke [12-15]. In addition, ZnO is added as a stabilizer, primarily to neutralize any acid formed as the composition ages. Linseed oil is used both as a lubricant during compression and as a binder to hold the ingredients together after compression of the composition. LO can also be replaced by a polymer or rubber compound, such as epoxy resin (EP) [16, 17], hydroxyl terminated polybutadiene (HTPB) [4], polyvinyl chloride (PVC) [18], polystyrene (PS) [18], polysulfide rubber (PSR) [2], butyl rubber (IIR) [19], *etc*.

The smoke markers with RP can be loaded by two different methods. The first and most common method is the tamp-casting method, all the ingredients are usually mixed well in a suitable mixer and then pressed into a container used as a smoke marker. Finally, the thermal curing process is done in an inert atmosphere. The preferred amount of resin binder used in this method is in the range of about 10-18% [16]. Another method is the pour-casting method. The required amount of binder must be as high as 25-30%, because fine RP has a large surface area per unit volume and requires a large amount of binder to wet the RP. Our research group [4] has studied the preparation and characterization of pour-casting RP smoke agent with HTPB as binder. However, the effect of different oxidizers on combustion performance has not been explored.

This study continued the previous research of our research group to explore the optimum composition and characteristics of pour-casting RP smoke agents with different oxidizers. Taguchi experimental design method was adopted to design the experimental conditions of three RP smoke agents with KNO_3, MnO_2 or SiO_2 as the oxidizer, and the vacuum pour-casting method was used

to prepare the scaled-down test samples. The combustion phenomena of these scaled-down test samples were recorded by the visual-image capture system, and the ignition and combustion temperatures were measured by the temperature measurement system. The burning rate was selected as the quality characteristic to analyze the optimum parameter combinations for obtaining the minimum average burning rate. Subsequently, the uniformity of composition distribution, hardness and mechanical strength of three scaled-down test samples prepared with the optimum parameter combination were observed and measured by scanning electron microscopy coupled with energy dispersive spectroscopy, hardness tester and tensile testing machine. In addition, the vacuum stability tester was used to determine the stability, and the smoke density test chamber was employed to measure the specific optical density of smoke generated by test samples. Finally, three full-size RP smoke candles with KNO_3, MnO_2 or SiO_2 as the oxidizer were prepared, and their combustion performance was actually measured and compared with the smoke candle in the MK 58 smoke marker.

2 Materials and Methods

2.1 Materials

Industrial-grade RP with a purity of >98% and a particle size of about 75 μm was obtained from the 202nd Arsenal in Taiwan. Industrial-grade magnesium (Mg) powder with a purity of >98% was provided by Johnson & Annie Co., Ltd. in Taiwan. Reagent-grade potassium nitrate (KNO_3) with a purity of 99.0%, manganese oxide (MnO_2) with a purity of 99.0% and silicon dioxide (SiO_2) with a purity of 99.9% were purchased from Sigma Aldrich and used as the oxidizers. Zinc oxide (ZnO) with a purity of 99.7% was purchased from Echo chemical Co., Ltd. in Taiwan and used as a stabilizer. The binder system consisted of hydroxyl-terminated polybutadiene (HTPB)/dioctyl adipate (DOA) and was cured by isophorone diisocyanate (IPDI). HTPB, DOA and IPDI were obtained from the Chemical Systems Research Division of National Chung Shan Institute of Science and Technology (NCSIST) in Taiwan.

2.2 Design of experimental conditions

The pyrotechnic composition of MK 58 smoke marker was adopted as a reference formula [20]. Taguchi analysis method is one of the most widely used design methods [21, 22], which was used in this study to design the experimental conditions. Firstly, RP, Mg, ZnO and oxidizer (KNO_3, MnO_2 or SiO_2) were mixed well as a RP mixture, then HTPB was used as a binder to consolidate

the RP mixture. Finally, DOA and IPDI were additionally added as plasticizer and curing agent, respectively. The experimental layout used the Taguchi $L_9(3^4)$ orthogonal array with four control factors and three levels. Four control factors were selected, including mass ratio of oxygen content in oxidizer to RP mixture, RP content in RP mixture, mass ratio of RP mixture to HTPB and additional amount of DOA, each at three levels. The control factors and levels of the Taguchi experiments using KNO_3 as the oxidizer are shown in Table 1. The above four factors were assigned to the $L_9(3^4)$ orthogonal array containing nine experimental conditions as shown in Table 2. In addition, the contents of ZnO and Mg in the RP mixture were fixed at 3 and 8 g, respectively. The NCO/OH ratio (R value) of IPDI to HTPB was set at 1.6, and the curing temperature was set at 50 °C. The ingredients of all formulations (A1-A9) are listed in Table 3. Similarly, the control factors and levels of the Taguchi experiments using MnO_2 and SiO_2 as the oxidizers are shown in Tables 4 and 5, respectively.

Table 1. Control factors and levels of Taguchi experiments using KNO_3 as oxidizer

Control factor	Level		
	1	2	3
A. Oxygen content of KNO_3 in RP mixture [%]	11	13	15
B. RP content in RP mixture [g]	51	52	53
C. Weight ratio of RP mixture to HTPB	85:15	86:14	87:13
D. Additional amount of DOA [wt.%]	3.0	3.5	4.0

Table 2. $L_9(3^4)$ orthogonal array of Taguchi experiments using KNO_3 as oxidizer

Exp. No.	Oxygen content of KNO_3 in RP mixture [%]	RP content in RP mixture [g]	Weight ratio of RP mixture to HTPB	Additional amount of DOA [wt.%]
A1	11	51	85:15	3.0
A2	11	52	86:14	3.5
A3	11	53	87:13	4.0
A4	13	51	86:14	4.0
A5	13	52	87:13	3.0
A6	13	53	85:15	3.5
A7	15	51	87:13	3.5
A8	15	52	85:15	4.0
A9	15	53	86:14	3.0

Table 3. Composition of formulations based on Taguchi experiments using KNO_3 as oxidizer

Exp. No.	Formulation ingredients						
	RP [g]	KNO_3 [g]	ZnO [g]	Mg [g]	HTPB [g]	IPDI [g]	DOA [g]
A1	51.00	27.78	3.00	8.00	15.84	3.17	2.02
A2	52.00	27.78	3.00	8.00	14.78	3.69	1.88
A3	53.00	27.78	3.00	8.00	13.71	4.22	1.74
A4	51.00	32.83	3.00	8.00	15.44	4.41	1.96
A5	52.00	32.83	3.00	8.00	14.32	3.30	1.82
A6	53.00	32.83	3.00	8.00	17.09	3.99	2.17
A7	51.00	37.88	3.00	8.00	14.92	4.02	1.90
A8	52.00	37.88	3.00	8.00	17.80	4.75	2.26
A9	53.00	37.88	3.00	8.00	16.59	3.55	2.11

Table 4. Control factors and levels of Taguchi experiments using MnO_2 as oxidizer

Control factor	Level		
	1	2	3
A. Oxygen content of MnO_2 in RP mixture [wt.%]	13	14	15
B. RP content in RP mixture [g]	48	49	50
C. Weight ratio of RP mixture to HTPB	84:16	86:14	88:12
D. Additional amount of DOA [wt.%]	3.5	4.0	4.5

Table 5. Control factors and levels of Taguchi experiments using SiO_2 as oxidizer

Control factor	Level		
	1	2	3
A. Oxygen content of SiO_2 in RP mixture [%]	15	16	17
B. RP content in RP mixture [g]	49	50	51
C. Weight ratio of RP mixture to HTPB	85:15	86:14	87:13
D. Additional amount of DOA [wt.%]	2.0	2.5	3.0

2.3 Preparation of test samples

The scaled-down test samples of different formulations were processed into cylindrical pellets with a diameter of 15.0 ±0.1 mm and a length of 70.0 ±0.1 mm by the vacuum pour-casting process. The schematic diagram of the preparation procedure is shown in Figure 1. Firstly, Mg, oxidizer (KNO_3, MnO_2 or SiO_2) and ZnO were weighed separately according to the proportion used in formulation and mixed carefully in a plastic container. The binder was prepared by mixing

certain amounts of HTPB and DOA in a glass container. The above binder and mixture were sequentially poured into a single planetary vacuum defoaming mixer and stirred for 20 min at room temperature. Afterwards, a certain amount of RP was carefully added into the previous mixer and continuously stirred for 20 min. Finally, IPDI was added into the mixer and continuously stirred for 10 min to form a well-mixed viscous mixture. Subsequently, this viscous mixture was poured into the moulds by vacuum pour-casting method, and then the filled moulds were transferred to an vacuum oven and the filler was cured at 50 °C for a predetermined time. After finishing the curing process, the moulds were took out from the oven, the cured products were demoulded and lightly sanded the lateral surfaces to prepare the scaled-down test samples. The full-size RP smoke candles were also prepared by the vacuum pour-casting process, and the preparation steps were the same as those of the scaled-down test samples. The vacuum pour-casting tool was assembled by our laboratory, as shown in Figure 2, and the preparation process of the smoke candle is shown in Figure 3. The prepared smoke candle had a diameter of 40 mm and a length of 390 mm, which was the same size as the smoke candle in the MK 58 smoke marker [20].

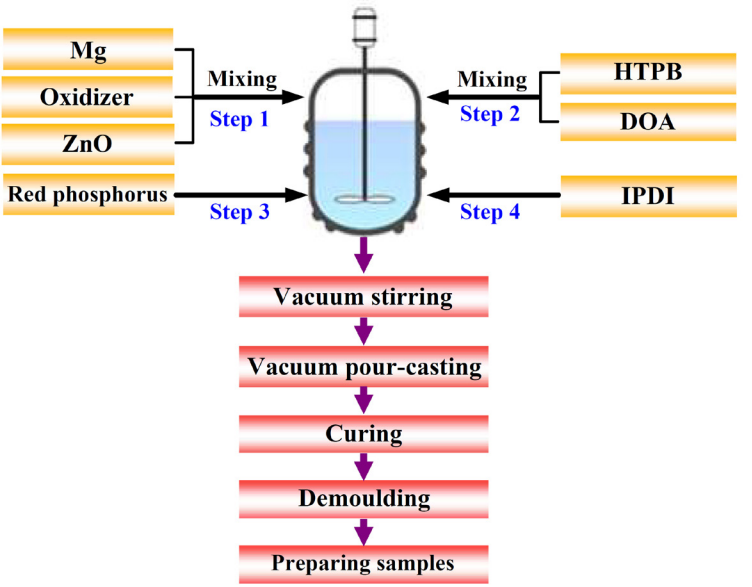

Figure 1. Schematic diagram of preparation procedure of test samples

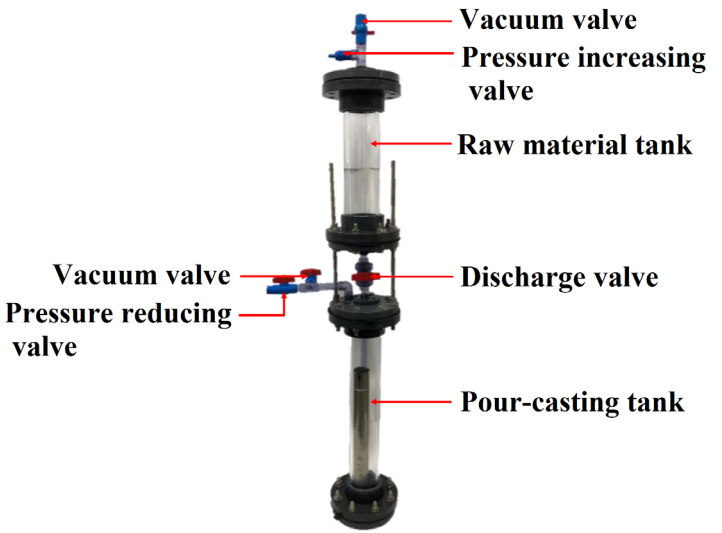

Figure 2. Photo of vacuum pour-casting tool

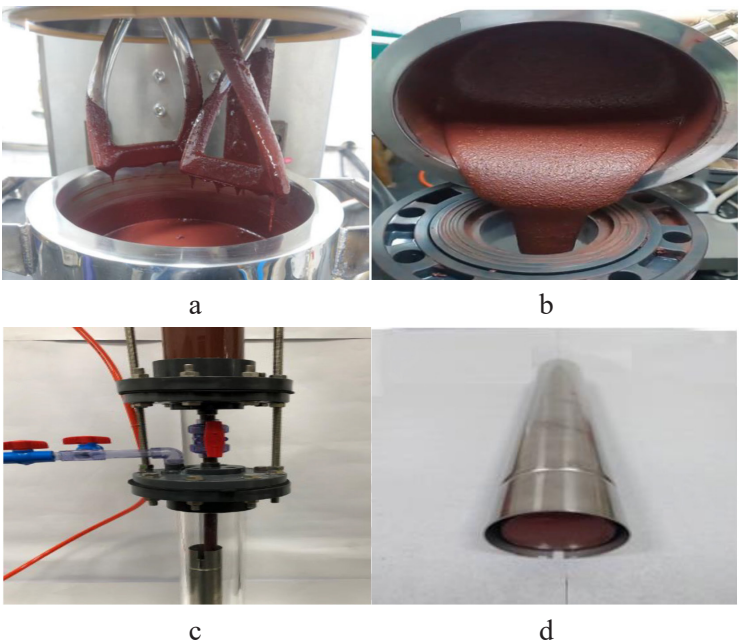

Figure 3. Preparation process of the smoke candle: mixing ingredients by using single planetary vacuum defoaming mixer (a), pouring the prepared mixture into vacuum pour-casting tool (b), preparing smoke candle by vacuum pour-casting (c) and curing in vacuum oven (d)

2.4 Apparatus and procedures

2.4.1 Combustion performance test

For the combustion performance test of the scaled-down test samples, the test sample was packed into a stainless steel tube, ignited by the electrical heating wire, and the temperature change during the combustion process was measured by two thermocouples located near the top and middle of the tube. The schematic diagram of the combustion performance test configuration is shown in Figure 4. The temperature measurement system consisted of two thermocouples, a signal processor and a PC-based data acquisition system. The thermocouple used was type K (chromel/alumel) with a wire diameter of 0.127 mm and had good dynamic response capability. The signal processor included a signal receiver and a filter amplifier. The data acquisition system had a resolution of approximately 0.015 °C and a sampling rate of 20 kHz. In addition, the phenomena of ignition, combustion and smoke generation were recorded by a visual-image capture system consisting of a digital video camera and a digital-image processing equipment. The digital video camera could shoot 30 fps. The digital-image processing equipment was connected with the digital video camera through an image acquisition card, and the captured video was edited through an image processing software to evaluate the burning rate. For the combustion performance test of the prepared smoke candles, the burning time was measured by using an ignition system and a visual-image capture system.

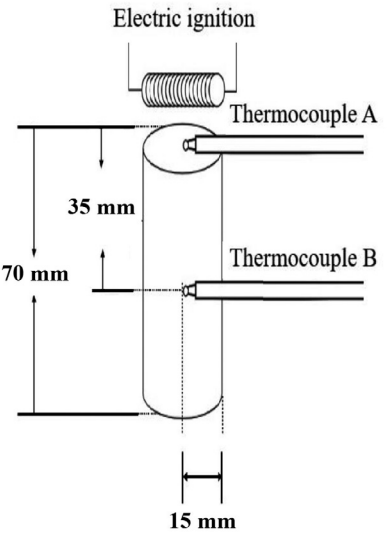

Figure 4. Schematic diagram of combustion performance test configuration for scaled-down test samples

2.4.2 Characteristics measurement

The uniformity of composition distribution, hardness and mechanical strength of the scaled-down test samples were observed and measured by scanning electron microscopy coupled with energy dispersive spectroscopy (SEM-EDS, JEOL JSM-6700F), hardness tester (HT, S.E.A.T. Industry Technology Co., Ltd. MET-DHG-A) and tensile testing machine (TTM, Wagner Instruments Chatillon TCD 200).

2.4.3 Stability test

The stability of the scaled-down test samples was determined by vacuum stability tester (VST, assembled by our laboratory) according to MIL-STD-1751A method 1063 [23]. The test sample with a weight of 5 g was placed in a glass tube and closed by a stopper with pressure and temperature transducers. The amount of gas generated by thermal decomposition of the test sample was measured under vacuum at 100 °C for 48 h. The maximum gas release required by the MILSTD-1751A standard is not to exceed 2 mL/g. The gas volume released in this test is a valid measure of the material stability [24].

2.4.4 Smoke density test

The specific optical density of the smoke generated by the test samples of RP smoke agent was evaluated according to the ASTM E662 test specification [25] using smoke density test chamber (SDTC, Fire testing technology Ltd. NBS SDTC). The RP smoke agent was processed into thin sheets with a size of 76.2×76.2×0.5 mm as the test samples. The test sample was mounted in the closed chamber and exposed vertically to an electric radiant heat source rated at 2.5 W/cm^2 for a maximum duration of 20 min. A light beam was then shone through the closed chamber. During this time, the photometric system was used to record the light transmittance values to determine the specific optical density. The measured data was presented in the form of a specific optical density versus time curve to determine the maximum value of the specific optical density.

3 Results and Discussion

3.1 Analysis and verification of Taguchi experiments

The combustion experiments of nine scaled-down test samples with KNO_3 as the oxidizer were carried out, and the data reported for each experiment were the average of three repeated experiments, and then the influence of each operating parameter on the burning rate were analyzed. A series of consecutive images of the combustion phenomenon captured by the digital video camera for Exp. No. A1 are shown in Figure 5. It is found that the total burning time is about 155 s, and the average burning rate can be calculated to be about 0.452 mm/s. Figure 6 demonstrates the corresponding temporal evolutions of the temperatures measured by two thermocouples located near the top and middle of test sample during the combustion process. The ignition temperature and combustion temperature are 228 and 543 °C, respectively. All experimental results of Taguchi $L_9(3^4)$ orthogonal array used for the combustion tests of the scaled-down test samples with KNO_3 as the oxidizer are listed in Table 6. These experimental results were future converted into signal-to-noise (S/N) ratios to quantify the effect of noise factors on the quality characteristic [26-29]. In this study, the average burning rate was selected as the quality characteristic. The analysis of average burning rate used smaller-the-better type, which meant that a smaller value indicated a better quality characteristic. The range and contribution rank of each factor for average burning rate of the scaled-down test samples with KNO_3 as the oxidizer are listed in Table 7. The target values of different levels on each factor are the arithmetic average of target values corresponding to each level. The range represents the difference between maximum and minimum of the target values on each factor, and the rank indicates the order of influence of each factor on this quality characteristic. The influence trend of the four factors on the average burning rate is shown in Figure 7. Levels A1, B3, C2 and D3 have minimum average burning rates for factors such as oxygen content of KNO_3 in RP mixture, RP content in RP mixture, weight ratio of RP mixture to HTPB and additional amount of DOA, respectively. Based on above analysis, the minimum average burning rate may be found on the condition that oxygen content of KNO_3 in RP mixture is 11 wt.%, RP content in RP mixture is 53 g, weight ratio of RP mixture to HTPB is 86:14, and additional amount of DOA is 4.0 wt.%. It is also found that the order of influence of various factors on this quality characteristic is oxygen content of KNO_3 in RP mixture (factor A) > weight ratio of RP mixture to HTPB (factor C) > RP content in RP mixture (factor B) > Additional amount of DOA (factor D). The oxygen content of KNO_3 in RP mixture has the greatest effect.

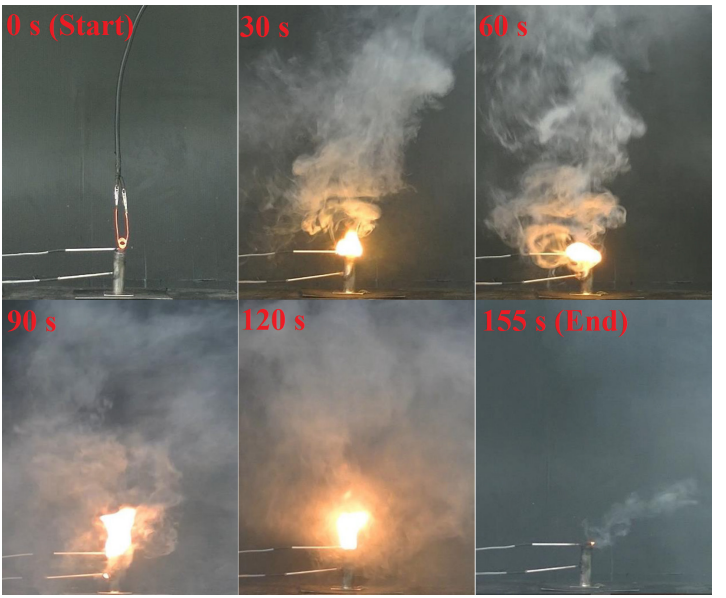

Figure 5. A series of consecutive images of combustion phenomenon captured by digital video camera for Exp. No. A1

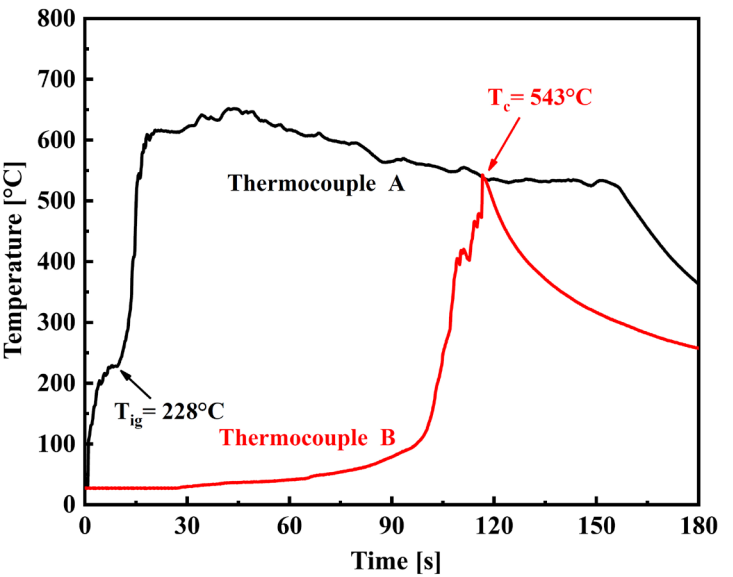

Figure 6. Temporal evolutions of temperatures measured by two thermocouples located near top and middle of test sample for Exp. No. A1

Table 6. Experimental results of Taguchi $L_9(3^4)$ orthogonal array used for combustion tests of scaled-down test samples with KNO_3 as oxidizer

Exp. No.	A1	A2	A3	A4	A5	A6	A7	A8	A9
Burning time [s]	155	163	148	131	84	154	63	91	121
Average burning rate [mm/s]	0.452	0.429	0.473	0.534	0.833	0.455	1.111	0.769	0.579
Ignition temperature [°C]	228	226	240	248	266	235	286	264	252
Combustion temperature [°C]	543	514	562	589	655	547	722	645	605

Table 7. Range and contribution rank of each factor for average burning rate of scaled-down test samples with KNO_3 as oxidizer (unit: mm/s)

Level	Control factors			
	A (Oxygen content of KNO_3 in RP mixture)	B (RP content in RP mixture)	C (Weight ratio of RP mixture to HTPB)	D (Additional amount of DOA)
1	0.451	0.692	0.559	0.621
2	0.609	0.678	0.515	0.658
3	0.813	0.503	0.799	0.594
Range	0.361	0.189	0.284	0.064
Rank	1	3	2	4

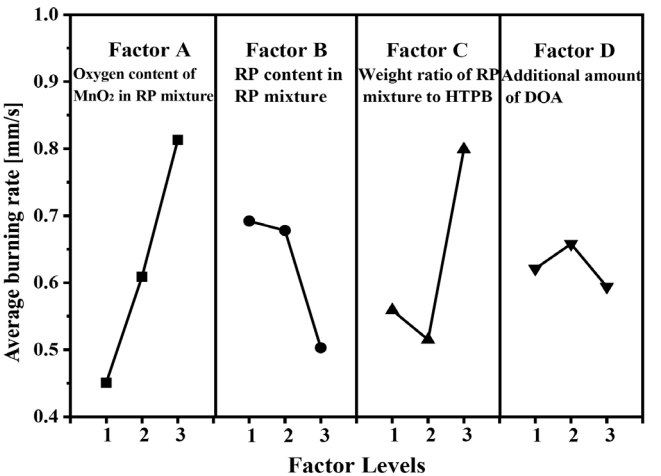

Figure 7. Influence trend of four factors on average burning rate of scaled-down test samples using KNO_3 as oxidizer

The additional confirmation experiments were carried out to verify the applicability of the optimum parameters identified by Taguchi analysis method. The optimum design factor for the minimum average burning rate of the scaled-down test samples with KNO_3 as the oxidizer is the A1B3C2D3 parameter combination. The experiment was repeated three times under the same test condition, and the average value of the results was taken. The results of all confirmation experiments are listed in Table 8. The experimental results reveal that the average burning rate of the scaled-down test sample with KNO_3 as the oxidizer under the A3B3C3D2 parameter combination is smaller than that of other parameter combinations tested in this study. Taguchi analysis method successfully predicted the optimum parameter combination to obtain the minimum average burning rate. Based on the above experimental and analytical results, the minimum average burning rate of the scaled-down test sample with KNO_3 as the oxidizer is 0.354 mm/s, and the corresponding ignition and combustion temperatures are 222 and 492 °C, respectively.

Table 8. Results of verification experiments for combustion tests of scaled-down test samples with KNO_3 as oxidizer

Optimum parameter combinations	Exp. No.	Burning time [s]	Average burning rate [mm/s]	Ignition temperature [°C]	Combustion temperature [°C]
A1B3C2D3	B1	195	0.359	226	498
	B2	197	0.355	224	495
	B3	201	0.348	217	484
	Average value	198	0.354	222	492

The same analytical method was also used for the scaled-down test samples with MnO_2 or SiO_2 as the oxidizer. The optimum parameter combination for the scaled-down test sample with MnO_2 as the oxidizer is A1B3C2D2, that is, oxygen content of MnO_2 in RP mixture is 13 wt.%, RP content in RP mixture is 50 g, weight ratio of RP mixture to HTPB is 86:14, and additional amount of DOA is 4.0 wt.%. The confirmation experiment results indicate that the minimum average burning rate is 0.281 mm/s, and the corresponding ignition and combustion temperatures are 273 and 478 °C, respectively. For the scaled-down test sample with SiO_2 as the oxidizer, the optimum parameter combination is A3B2C1D3, that is, oxygen content of SiO_2 in RP mixture is 17 wt.%, RP content in RP mixture is 50 g, weight ratio of RP mixture to HTPB is 85:15, and additional amount of DOA is 3.0 wt.%. The minimum average burning rate is 0.238 mm/s, and

the corresponding ignition and combustion temperatures are 313 and 413 °C, respectively. The optimum parameter combinations and burning characteristics for three scaled-down test samples with different oxidizers are summarized and listed in Table 9. Comparing three sets of scaled-down test samples with different oxidizers, it can be seen that the average burning rate of the test sample with KNO_3 as the oxidizer is higher than that of the other two test samples with MnO_2 or SiO_2 as the oxidizer. In addition, The test sample with KNO_3 as the oxidizer has a lower ignition temperature and a higher combustion temperature than the other two test samples with MnO_2 or SiO_2 as the oxidizer.

Table 9. Optimum parameter combinations and burning characteristics for three scaled-down test samples with different oxidizers

Oxidizer type	Optimum parameter combination	Burning time [s]	Average burning rate [mm/s]	Ignition temperature [°C]	Combustion temperature [°C]
KNO_3	A1B3C2D3	198	0.354	222	492
MnO_2	A1B3C2D2	249	0.281	273	478
SiO_2	A3B2C1D3	294	0.238	313	413

3.2 Characteristics analysis

The uniformity of composition distribution of the above three scaled-down test samples prepared with the optimum parameter combination was observed and analyzed by SEM-EDS. The test specimen was taken from the central region of the longitudinal section of the scaled-down test sample. The SEM and EDS images of the test specimen taken from the scaled-down test sample with KNO_3 as the oxidizer are shown in Figure 8. It can be seen from the SEM image that the structure of the test specimen is uniform and dense without cracks and pores. The structural defects of the prepared samples can be avoided by adopting the vacuum pour-casting process. The corresponding EDS elemental mapping data of P, Mg, K and Zn elements indicate that the test specimen contains 71.8 At% P, 14.4 At% Mg, 12.2 At% K and 1.6 At% Zn, which is very close to the composition of the formulation (72.8 At% P, 14.0 At% Mg, 11.7 At% K and 1.5 At% Zn). This also means that the prepared scaled-down test sample has a uniform composition distribution. The method described above was also applied to the other two test specimens taken from the scaled-down test samples with MnO_2 or SiO_2 as the oxidizer, and the results indicate that the two test specimens also have a uniform composition distribution.

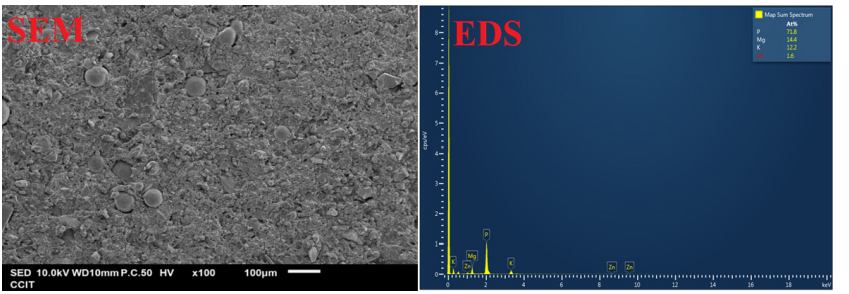

Figure 8. SEM and EDS images of test specimen taken from scaled-down test sample with KNO_3 as oxidizer

The hardness of above three scaled-down test samples prepared with the optimum parameter combination was measured by hardness tester on the Shore A scale. The transient hardness evolutions of three test samples during curing process are shown in Figure 9. It is found that the maximum hardness values of three scaled-down test samples with KNO_3, MnO_2 or SiO_2 as the oxidizer are 68.5, 64.2 and 67.2, respectively, which means that their hardness level is similar to that of hard rubber. Generally speaking, the materials with higher hardness have lower plastic deformation capacity, which can easily cause structural damage and cracking during storage and transportation. In addition, it is noteworthy that the curing time of the scaled-down test sample with KNO_3 as the oxidizer is significantly longer than that of the scaled-down test samples with MnO_2 or SiO_2 as the oxidizer.

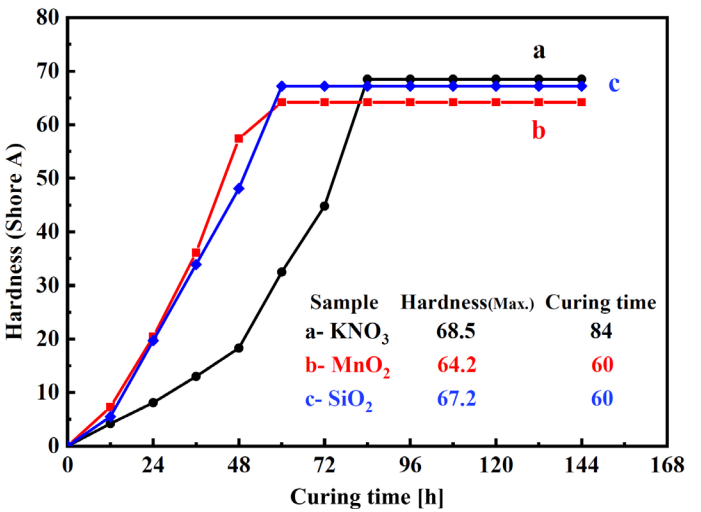

Figure 9. Transient hardness evolutions of scaled-down test samples with KNO_3, MnO_2 or SiO_2 as oxidizer during curing process

The mechanical strength of above three scaled-down test samples prepared with the optimum parameter combination was measured by tensile testing machine according to the ASTM 1708-18 standard [30]. The dumbbell-shaped specimens with a length of 38 mm, a width of 15 mm, and a cross-sectional dimension of 5×12 mm^2 in the narrowed middle region were cut from the prepared test samples. The specimen was strained at a crosshead speed of 50 mm/min, and the values of stress and strain at the break were determined. Each experiment was repeated three times and the average value of the results was taken. Figure 10 displays the stress versus strain curves of the scaled-down test samples with KNO_3, MnO_2 or SiO_2 as the oxidizer (Exp. Nos. C1, D1 and E1). The results of all experiments are listed in Table 10. The average maximum stresses of three scaled-down test samples with KNO_3, MnO_2 or SiO_2 as the oxidizer are 1.83, 1.68 and 1.99 MPa, respectively, and the corresponding average maximum strains are 7.10, 16.77 and 9.73%, respectively. In general, higher maximum stress means greater strength, and higher maximum strain means greater ductility. The experimental results show that three scaled-down test samples have sufficient strength and ductility to avoid structural damage caused by unexpected collision forces.

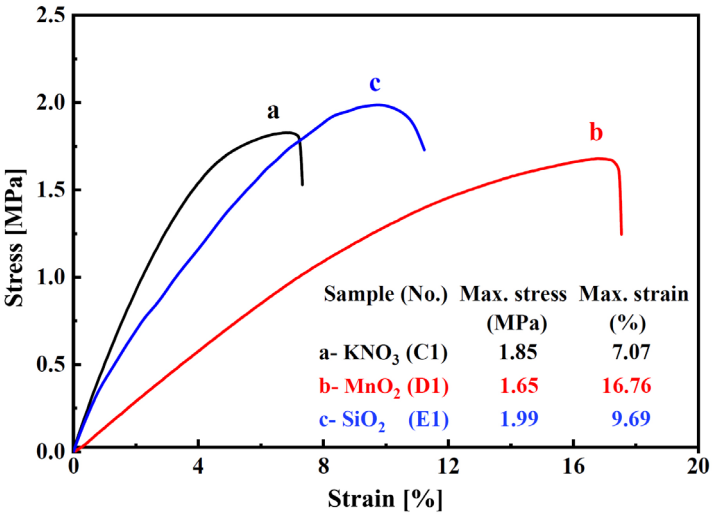

Figure 10. Stress versus strain curves of scaled-down test samples with KNO_3, MnO_2 or SiO_2 as oxidizer (Exp. Nos. C1, D1 and E1)

Table 10. Results of mechanical strength tests for three scaled-down test samples with different oxidizers

Oxidizer type	Exp. No.	Max. stress [MPa]	Max. strain [%]
KNO_3	C1	1.85	7.07
	C2	1.84	7.12
	C3	1.80	7.11
	Average value	1.83	7.10
MnO_2	D1	1.65	16.76
	D2	1.72	16.79
	D3	1.67	16.76
	Average value	1.68	16.77
SiO_2	E1	1.99	9.69
	E2	1.98	9.76
	E3	2.00	9.74
	Average value	1.99	9.73

3.3 Stability analysis

The stability of above three scaled-down test samples prepared with the optimum parameter combination was determined by vacuum stability tester according to the standard established by MIL-STD-1751A. The advisory criterion for testing is that the amount of gas released by the test sample should not exceed 2 mL/g. The pressure-time curves of three test samples are shown in Figure 11. The amounts of gas released from three scaled-down test samples with KNO_3, MnO_2 or SiO_2 as the oxidizer are 0.29, 0.21 and 0.13 ml/g, respectively. Since the amount of gas released does not exceed 2mL/g, it indicates that these compositions have good stability.

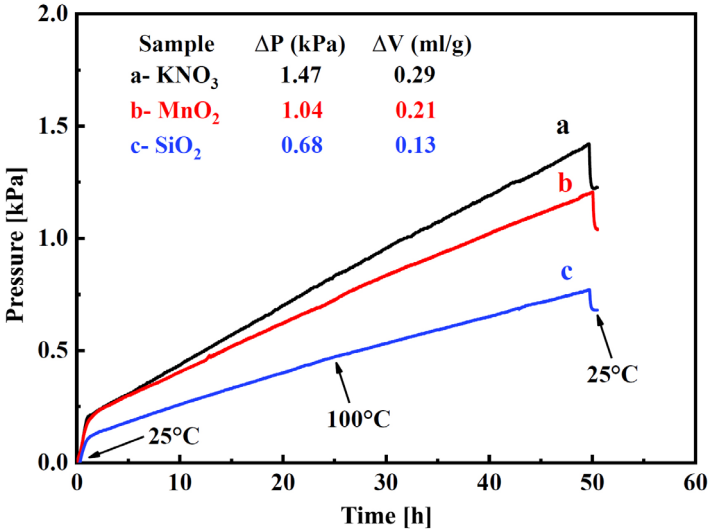

Figure 11. Pressure-time curves of scaled-down test samples with KNO_3, MnO_2 or SiO_2 as oxidizer obtained by VST with 100 °C/48 h

3.4 Smoke density analysis

The specific optical density of the smoke generated by the test samples of three RP smoke agents prepared with the optimum parameter combination was measured by smoke density test chamber. Figure 12 shows the temporal evolutions of the specific optical density (Ds) of the smoke generated by the test samples of three RP smoke agents with KNO_3, MnO_2 or SiO_2 as the oxidizer. It is found that the maximum smoke density occurs at about 30 seconds after ignition. The maximum Ds (Ds_{max}) values of three RP smoke agents with KNO_3, MnO_2 or SiO_2 as the oxidizer are 292.2, 311.1 and 239.6, respectively, and the corresponding average Ds (Ds_{avg}) values are 239.1, 252.4 and 208.8, respectively. Among them, it is noted that the smoke densities generated by the RP smoke agents with KNO_3 or MnO_2 as the oxidizer are similar, but they are higher than the smoke density generated by the RP smoke agent with SiO_2 as the oxidizer.

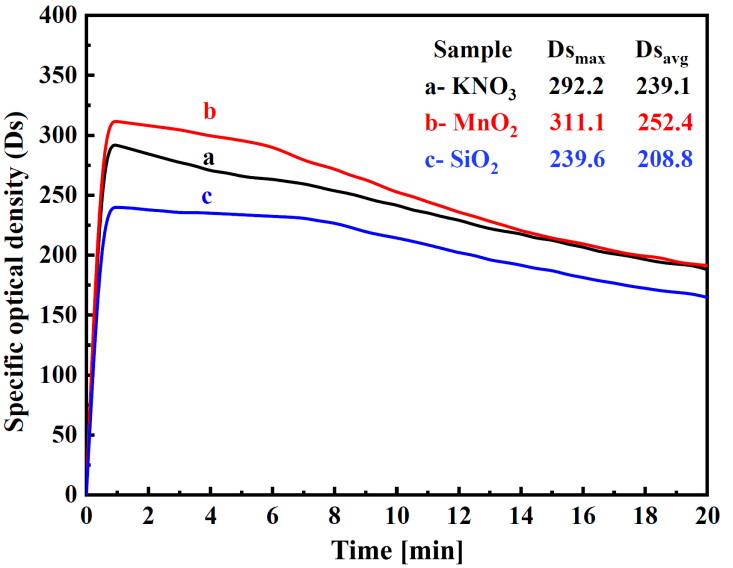

Figure 12. Temporal evolutions of specific optical density (Ds) of smoke generated by RP smoke agents with KNO_3, MnO_2 or SiO_2 as oxidizer

3.5 Combustion performance analysis of full-size RP smoke candle

The combustion performance tests of three full-size RP smoke candles with KNO_3, MnO_2 or SiO_2 as the oxidizer were carried out in the open space on our campus, the combustion phenomenon was recorded by the visual-image capture system, and the ambient temperature, relative humidity and average wind speed of the location were completely marked. A series of consecutive images of the combustion phenomenon of the full-size RP smoke candle with KNO_3 as the oxidizer taken by the digital video camera are shown in Figure 13. The smoke-generating time is about 18 min and 18 s, and the height of the smoke layer is more than 10 m above the ground. The similar experimental conditions were also used for the full-size RP smoke candles with MnO_2 or SiO_2 as the oxidizer. The experimental results indicate that the smoke-generating time are 26 min 54 s and 36 min 15 s, respectively. It is known that MK 58 smoke marker has two smoke candles, and the smoke-generating time of each smoke candle is about 20 to 30 min. The combustion performance of the full-size RP smoke candles with KNO_3 or MnO_2 as the oxidizer is close to that of the smoke candle in the MK 58 smoke marker. However, the full-size RP smoke candle with SiO_2 as the oxidizer has a longer smoke-generating time but a lower smoke density than the smoke candle in the MK 58 smoke marker.

Figure 13. A series of consecutive images of combustion phenomenon taken by digital video camera for full-size RP smoke candle with KNO_3 as oxidizer

4 Conclusions

This study used experimental methods to explore the optimum composition and characteristics of three pour-casting RP smoke agents with KNO_3, MnO_2 or SiO_2 as the oxidizer. Based on the experimental and analytical results, the following conclusions can be obtained:

- Taguchi analysis method successfully predicts the optimum parameter combination to obtain the minimum average burning rate of three scaled-down test samples with KNO_3, MnO_2 or SiO_2 as the oxidizer. The optimum parameter combination for the scaled-down test sample with KNO_3 as the oxidizer is as follows: oxygen content of KNO_3 in RP mixture is 11 wt.%, RP content in RP mixture is 53 g, weight ratio of RP mixture to HTPB is 86:14 and additional amount of DOA is 4.0 wt.%. The optimum parameter combination for the scaled-down test sample with MnO_2 as the oxidizer is as follows: oxygen content of MnO_2 in RP mixture is 13 wt.%, RP content in RP mixture is 50 g, weight ratio of RP mixture to HTPB is 86:14, and additional amount of DOA is 4.0 wt.%. The optimum parameter combination for the scaled-down test sample with SiO_2 as the oxidizer is as follows: oxygen content of SiO_2 in RP mixture is 17 wt.%, RP content in RP mixture is 50 g, weight ratio of RP mixture to HTPB is 85:15, and additional amount of DOA is 3.0 wt.%.
- The characteristics analysis shows that above three scaled-down test samples prepared with the optimum parameter combination have uniform composition distribution, proper hardness, and sufficient strength and ductility to avoid structural damage caused by unexpected collision forces.
- The vacuum stability tests indicate that the amount of gas released from above three scaled-down test samples prepared with the optimum parameter combination does not exceed 2mL/g. These compositions have good stability according to MIL-STD-1751A standard.
- The smoke density tests show that the smoke densities generated by the test samples with KNO_3 or MnO_2 as the oxidizer are similar, but they are higher than the smoke density generated by test samples with SiO_2 as the oxidizer.
- The combustion performance of the full-size RP smoke candles with KNO_3 or MnO_2 as the oxidizer is close to that of the smoke candle in the MK 58 smoke marker. However, the full-size RP smoke candle with SiO_2 as the oxidizer has a longer smoke-generating time but a lower smoke density than the smoke candle in the MK 58 smoke marker. In addition, the RP smoke candles prepared by vacuum pour-casting technology can be used to make smoke marker and meet performance requirements.

Acknowledgements

The authors thank the 202nd Arsenal in Taiwan for funding the study and providing experimental ingredients. The authors would also like to thank Professors Tsao-Fa Yeh and Chyi-Ching Hwang for their useful suggestions regarding data processing.

References

[1] Collins, P.J.D. Overview on Red Phosphorus - An International Perspective (Invited). *Proc. 27th Int. Pyrotechnics Sem.*, Colorado, USA, **2000**, 191-206.
[2] Artz, G.D. Red Phosphorus Castable Smoke Producing Composition. Patent US 3650856, **1972**.
[3] Mishra, P.K. Role of Smokes in Warfare. *Def. Sci. J.* **1994**, *44*(2): 173-179; https://doi.org/10.14429/DSJ.44.4166.
[4] Yang, T.M.; Tseng, H.W.; Li, J.S., Lu, K.T.; Ku, H.C.; Lin, T.W. Preparation and Characterization of Pour-Casting Red Phosphorus Smoke Agents with HTPB as Binder. *Propellants Explos. Pyrotech.* **2020**, *46*(12): 1784-1799; https://doi.org/10.1002/prep.202100229.
[5] Stoenescu, L. *Colored Pyrotechnic Smoke-producing Composition.* Patent US 2014/0238258 A1, **2014**.
[6] Diviacchi, G.; Domanico, J.A.; May, J.E.; Redding, D.R. *Low Toxicity, Environmentally Friendly Violet Smoke Generating Compositions and Methods of Making the Same.* Patent US 10663272, **2020**.
[7] *Toxicity of Military Smokes and Obscurants: Volume 2*. National Research Council, Division on Earth and Life Studies, Commission on Life Sciences, Subcommittee on Military Smokes and Obscurants, Washington, DC, National Academies Press, **1999**.
[8] *Gunner's Mate 1 and C (NAVEDTRA 14110)*. (Bomar, J.; Null, R.; Wallace, J., eds.) Florida, Naval Education and Training Professional Development and Technology Center, **1996**.
[9] Niehaus, F.A.; Landstrom, B. *Performance Oriented Packaging Testing of Polystyrene Foam Container for MK 58 Marine Location Marker*. Indiana, Navel Weapons Support Center, **1991**.
[10] Montgomery, F.E. *A 1/10 Scale Pilot Plant for the Ecological Demilitarization of Mk 25 Marine Location Markers/Red Phosphorus Composition*. Indiana, Naval Weapons Support Center, **1977**.
[11] *Water Range Assessment for the VACAPES Range Complex.* Naval Facilities Engineering Command, Final report, Washington, D.C., U.S. Department of the Navy, **2010.**
[12] Liberman, T. *Smoke Composition and Method of Making Same.* Patent US 4841865, **1989**.

[13] Liberman, T. *Smoke Producing Composition for Pyrotechnic Markers, Method for the Production Thereof and Pyrotechnic Markers Containing Same.* Patent GB 2206343A, **1989**.
[14] Koch, E.C. Special Materials in Pyrotechnics: V. Military Applications of Phosphorus and Its Compounds. *Propellants Explos. Pyrotech.* **2008**, *33*(3): 165-176; https://doi.org/10.1002/ prep.200700212.
[15] Shaw, A.P.; Brusnahan, J.S.; Poret, J.C.; Morris, L.A. Thermodynamic Modeling of Pyrotechnic Smoke Compositions. *ACS Sustainable Chem. Eng.* **2016**, *4*(4): 2309-2315; https://doi.org/10.1021/acssuschemeng.5b01762.
[16] Douda, B.E. *White Smoke Composition Containing Red Phosphorous.* Patent US 3607472, **1971**.
[17] Knapp, C.A.; Wayne, N.J. *Red Phosphorous Smoke Producing Composition.* Patent US 4534810, **1985**.
[18] Cullis, C.F.; Hirschler, M.M.; Tao, Q.M. The Effect of Red Phosphorus on the Flammability and Smoke-producing Tendency of Poly(Vinyl Chloride) and Polystyrene. *Eur. Polym. J.* **1986**, *22*(2): 161-167; https://doi.org/10.1016/0014-3057(86)90112-6.
[19] Davies, N. *Red Phosphorus for Use in Screening SmokeCompositions*. Shrivenham, Royal Military College of Science Cranfield University, **1999**.
[20] *Standard Operating Procedure Manual for Loading, Assembly and Packaging of MK58 Smoke Marker (Edition 2.1)*. (in Chinese) 202nd Arsenal, Production and Manufacturing Center of the Armament Bureau, Ministry of National Defense, Taiwan, Republic of China, **2020**.
[21] Taguchi, S. *Taguchi Methods and QFD: Hows and Whys for Management*. American Supplier Institute, Michigan, **1987**, ISBN: 978-0-94-124304-9.
[22] Cochran, W.G.; Cox, G.M. *Experimental Design.* 2nd ed., John Wiley & Sons, New York, **1992**.
[23] *Department of Defense Test Method Standard: Safety and Performance Tests for the Qualification of Explosives (High explosives, Propellants, and Pyrotechnics)*. MIL-STD-1751A, U.S. Department of Defense, Virginia, **2001**.
[24] Barros, L.; Pinheiro, A.P.M.; Camara, J.E.; Iha, K. Qualification of Magnesium/Teflon/Viton Pyrotechnic Composition Used in Rocket Motors Ignition System. *J. Aerosp. Technol. Manage.* **2016**, *8*(2): 130-136; https://doi.org/10.5028/jatm.v8i2.596.
[25] *Standard Test Method for Specific Optical Density of Smoke Generated by Solid Materials*. ASTM E 662, ASTM International, West Conshohocken, USA, PA, **2012**.
[26] Li, J.S.; Chen, F.J.; Yang, H.W.; Lu, K.T. Study on Synthesis and Characterization of Primary Explosive KDNBF with Different Morphologies. *Propellants Explos. Pyrotech.* **2020**, *45*(8): 1313-1325; https://doi.org/10.1002/prep.202000052.
[27] Li, W.H.; Tseng, K.C.; Yang, T.M.; Li, J.S.; Lu, K.T. Optimization of Synthesis Parameters and Characterization of Green Primary Explosive Copper(I) 5-nitrotetrazolate (DBX-1). *Propellants Explos. Pyrotech.* **2020**, *45*(12): 1831-1840, https://doi.org/10.1002/prep.202000173.

[28] Yang, T.M.; Chang, Y.C.; Li, J.S.; Peng, C.H.; Lu, K.T. Combustion Synthesis of Green $Zn_{1-x}Co_xO$ Nanopowders and Their Application in Multi-Spectral Camouflage/Stealth Materials. *Mater. Express* **2021**, *11*(4): 492-505; https://doi.org/10.1166/mex.2021.1941.
[29] Yang, T.M.; Shih, C.W.; Hwang, C.C.; Lu, K.T. Composition Optimization and Characterization of Combustible Cartridge Cases with Polyvinyl Acetate (PVAc) as a Binder. *Mater. Express* **2022**, *12*(5): 713-725; https://doi.org/10.1166/mex.2022.2192.
[30] *Standard Test Method for Tensile Properties of Plastics by Use of Microtensile Specimens*. ASTM D1708-18, ASTM International, Pennsylvania, **2018**.

Authorship contribution statement

Jin-Shuh Li: conception, methods
Cheng-Hsiung Peng: performing the experimental part, performing the statistical analysis
Kai-Tai Lu: other contribution to the publication
Po-Han Chen: foundations, performing the experimental part

Submitted: February 17, 2025
Revised: March 25, 2026
First published online: March 31, 2026